

# Mechanism of Inhibition of HIV-1 Reverse Transcriptase by the Novel Broad-Range DNA Polymerase Inhibitor

*N*-{2-[4-(Aminosulfonyl)phenyl]ethyl}-2-(2-thienyl)acetamide<sup>†,‡</sup>

Alon Herschhorn, Iris Oz-Gleenberg, and Amnon Hizi\*

Department of Cell and Developmental Biology, Sackler School of Medicine, Tel Aviv University, Tel Aviv 69978, Israel

Received September 5, 2007; Revised Manuscript Received October 16, 2007

**ABSTRACT:** Employing a novel strategy, we have virtually screened a large library of compounds to identify novel inhibitors of the reverse transcriptase (RT) of HIV-1. Fifty-six top scored compounds were tested in vitro, and two of them inhibited efficiently the DNA polymerase activity of RT. The most effective compound, *N*-{2-[4-(aminosulfonyl)phenyl]ethyl}-2-(2-thienyl)acetamide (NAPETA), inhibited both RNA-dependent and DNA-dependent DNA polymerase activities, with apparent IC<sub>50</sub> values of 1.2 and 2.1 μM, respectively. This inhibition was specific to the RT-associated polymerase activity and did not affect the RNase H activity. NAPETA also inhibited two drug-resistant HIV-1 RT mutants as well as HIV-2 RT and other DNA polymerases. Kinetic analysis of RT inhibition indicated that the DNA polymerase activity of HIV-1 RT was inhibited in a classic noncompetitive manner with respect to dTTP, demonstrating a *K<sub>i</sub>* value of 1.2 μM. In contrast, the inhibition with respect to the RNA•DNA template was a mixed linear type with a *K<sub>i</sub>* value of 0.12 μM and was not affected by the order in which the template•primer and inhibitor were added to the reaction mixture. Gel shift and surface plasmon resonance analyses confirmed that NAPETA interfered with the formation of the RT•DNA complex (that is crucial for the polymerization activity) by reducing the affinity of RT for DNA, accounting at least partially for the inhibition. It is likely that NAPETA inhibited RT via a mechanism that is different from that of the classic non-nucleoside RT inhibitors used for treating AIDS/HIV patients and, thus, may serve as a lead compound for the development of novel anti-HIV drugs.

The reverse transcriptase (RT)<sup>1</sup> of human immunodeficiency virus type-1 (HIV-1) is an essential enzyme in the life cycle of this retrovirus. Upon infecting the target cell, RT copies the viral plus sense and single-stranded genomic

RNA into a double-stranded DNA. This complex reverse transcription process, which is common in all retroviruses, is catalyzed solely by RT and is mediated by the three activities of the enzyme. The two related RNA-dependent DNA polymerase (RDDP) and DNA-dependent DNA polymerase (DDDP) activities enable DNA synthesis of the viral genome, whereas the ribonuclease H (RNase H) activity concomitantly cleaves the viral RNA strand in the RNA•DNA heteroduplex. The resulting double-stranded DNA is transported into the infected cell nucleus, as part of a pre-integration complex, and is subsequently incorporated into the cellular DNA by the viral integrase (*I*).

Almost all inhibitors of HIV-1 RT can be grouped into two classes of potent compounds: nucleoside/nucleotide RT inhibitors (NRTIs) and non-nucleoside RT inhibitors (NNRTIs) (2). NRTIs are competitive inhibitors that are phosphorylated by cellular kinases and subsequently mimic normal nucleotides. Since NRTIs lack the 3'-OH group, their incorporation into the nascent DNA by RT blocks further addition of nucleotides and, hence, leads to termination of chain elongation. The NNRTIs are a variety of hydrophobic noncompetitive inhibitors that are presumed to bind specifically to a hydrophobic pocket located in the proximity of the DNA polymerase active site of the RT (3). Most NNRTIs are highly specific against HIV-1 RT with minimal effects on the closely related HIV-2 RT (4). Both classes of inhibitors are currently used in the therapy against HIV-1

<sup>†</sup> A. Hizi is the Incumbent of the Gregorio and Dora Shapira Chair for the Research of Malignancies. A. Herschhorn is supported by the Tel Aviv University president and rector scholarship for excellence.

<sup>‡</sup> This work was performed in partial fulfillment of the requirements for a Ph.D. degree by A. Herschhorn, Sackler Faculty of Medicine, Tel Aviv University.

\* To whom correspondence should be addressed: Department of Cell and Developmental Biology, The Sackler School of Medicine, Tel Aviv University, Tel Aviv 69978, Israel. Telephone: 972-36409974. Fax: 972-36407432. E-mail: ahizi@post.tau.ac.il.

<sup>1</sup> Abbreviations: RT, reverse transcriptase; RDDP, RNA-dependent DNA polymerase; DDDP, DNA-dependent DNA polymerase; RNase H, ribonuclease H; HIV, human immunodeficiency virus; NRTI, nucleoside/nucleotide reverse transcriptase inhibitor; NNRTI, non-nucleoside reverse transcriptase inhibitor; KM-1, 2-naphthalenesulfonic acid (4-hydroxy-7-[(5-hydroxy-6-[(4-cinnamylphenyl)azo]-7-sulfo-2-naphthalenyl)amino]carbonyl)amino-3-[(4-cinnamylphenyl)azo]; NAPETA, *N*-{2-[4-(aminosulfonyl)phenyl]ethyl}-2-(2-thienyl)acetamide; SDS, sodium dodecyl sulfate; SPR, surface plasmon resonance; PETT, phenylethylthiazolylthiourea; PDB, Protein Data Bank; MDBACEC, methyl 2-[(5,6-dimethyl-1,3-benzothiazol-2-yl)amino]carbonothioyl)-amino)-5-ethylthiophene-3-carboxylate; TSAO, [2',5'-bis-*O*-(*tert*-butyldimethylsilyl)-3'-spiro-5''-(4''-amino-1'',2''-oxathiole-2'',2''-dioxide)]-β-D-pentofuranosyl; EDC, 1-ethyl-3-[3-(dimethylamino)propyl]carbodiimide hydrochloride; NHS, *N*-hydroxysuccinimide; HBS, HEPES buffer saline; PERV, porcine endogenous retrovirus; Tf1, LTR retrotransposon Tf1; Taq, *Thermus aquaticus*; XTT, 2,3-bis(2-methoxy-4-nitro-5-sulfophenyl)-5-[(phenylamino)carbonyl]-2H-tetrazolium hydroxide; 2GP, 2-*O*-galloylpunicalin; AZT, 3'-azido-3'-deoxythymidine.

as part of the highly active antiretroviral therapy that targets simultaneously the RT, the viral protease, and most recently the cellular entry step of the virus (5).

The high specificity of the currently used NNRTIs in therapy poses a significant obstacle for their systemic use, as it usually reduces their efficacy against mutated variants of RT in the infectious viruses (6). Unfortunately, enzymes that serve as preferential targets for therapy are quite flexible, which means that they can tolerate mutations and still remain functionally active. This eventually leads to resistance, which develops rapidly during treatment, even when a combination of drugs is used. Consequently, intense efforts have been directed in recent years to find broad-spectrum novel NNRTIs inhibiting both wild-type and RT variants that are resistant to the currently used drugs. This intensive search has recently led to the discovery of several new highly efficient RT inhibitors, including TMC-125 (etravirine), GW678248, YM-215389, TMC-120 (dapivirine), and rilpivirine (7–10).

Additional inhibitors that block RT activities by new mechanisms have also been recently identified and offer different approaches to overcoming resistance. KM-1, which was initially designed to interact with the RT·DNA complex, inhibited various drug resistance mutants of RT (11). Unlike the classic NNRTIs, this compound does not bind the hydrophobic pocket but rather inhibits RT by lowering the affinity of the enzyme toward the nucleic acid substrate (12). Phosphonoformic acid, already approved by the FDA for clinical treatment, traps the pre-translocated state of HIV-1 RT and consequently prevents the forward motion of the enzyme during DNA synthesis (13). Indolopyridone-1 probably binds the RT nucleotide binding site and inhibits binding and incorporation of the next complementary nucleotide (14). Since the mechanism by which all these compounds inhibit RT is different from that of the classic NNRTIs (such as delaviridine, nevirapine, and efavirenz), it is reasonable to assume that they would inhibit variants of RT known to be resistant to the currently used drugs. Therefore, the identification of additional new inhibitors and elucidation of their mode of action are imperative for channeling new potent leads for further research and for developing new strategies to fight AIDS/HIV.

In this work, we present a novel approach for the identification of novel NNRTIs by virtually screening in silico an available chemical library against two different crystal structures of HIV-1 RT (PDB entries 1fk9 and 1dtq). Compounds that exhibited potential binding capacities for both structures were further tested in vitro for their inhibition of the enzymatic activity of HIV-1 RT, and the most effective one was further studied using several experimental systems for its mode of inhibition. The compound identified herein by us, NAPETA, could efficiently inhibit HIV-1 RT, and this activity was mediated by a mechanism that was different from that of most of the classic NNRTIs. Since this compound inhibited also other DNA polymerases, it will probably be difficult for drug-resistant RT mutants to evade this inhibitor.

## EXPERIMENTAL PROCEDURES

**Virtual Screening.** Docking a library of compounds into RT structures included three preliminary steps: (1) prepara-

tion of RT structures, (2) generation of an idealized binding site in each RT (a protomol), and (3) optimization of the conformation of each compound in the library.

(a) *Preparation of RT Structures.* PDB entries 1fk9 (15) and 1dtq (4) were downloaded from the Research Collaboratory for Structural Bioinformatics as a complex with a specific inhibitor (efavirenz and PETT-1 for these two RT structures, respectively). The inhibitors were removed from these structures, and missing hydrogen atoms were added to each one. (b) *Protomol Generation.* For each RT structure, the location of the original inhibitor was used to generate a protomol using the defaults setting of the Surflex program. As previously described (16), in this process, CH<sub>4</sub>, C=O, and NH molecular fragments are placed into the protein binding site in multiple positions and are optimized for interaction with the protein. High-scoring nonredundant fragments collectively form the protomol. (c) *Library Preparation.* The “diversity” library from Chembridge was downloaded as a structure data (sd) file, and each compound was energy-minimized with Omega (Openeye Software) into a single optimized conformation using the mmff94s force field (17). All compounds were saved in their optimized conformation in a mol2 file, which retains their spatial coordinates in space.

The 1fk9 RT structure, the generated protomol, and the compound-optimized library files were used as input for the docking process. Docking was performed by fragmenting each molecule and fitting the conformation of each fragment into the protomol to yield a spatial structure that maximizes the molecular similarity to the protomol. Ten top conformations for each compound were retrieved according to their score as output files. These included a log output file with the scores for each conformation and a structural output file with the coordinates for the suggested conformations. All retrieved compounds were then filtered from the log output file by using thresholds of 6 for score values, −2 for crash values, and 1 for polar values with the Filter program. Docking conformations of filtered top compounds were extracted from the structural output file with the Extract program (Filter and Extract are in-house programs, written in Perl to filter and extract, respectively, specific conformations of specific compounds from the results file; both are available upon request). This process was repeated with the 1dtq RT structure, but this time, only the top scored molecules from the 1fk9 docking were screened. Molecules were then ranked on the basis of their average scores over the two RT structures. Each was further analyzed visually with discovery studio visualizer 1.6 (Accelrys Software Inc.), and 56 of them were selected and purchased from Chembridge. Molecular properties were extracted from the Chembridge database (Hit2lead web site). The conformations of reference NNRTIs were docked in the same manner, and the molecular properties of these inhibitors were calculated using the molinspiration on-line calculator (<http://www.molinspiration.com/cgi-bin/properties>).

**Expression and Purification of RTs.** Recombinant wild-type p66/p51 HIV-1 RT, derived from the BH10 clone, was expressed in bacteria. This enzyme, which has a six-histidine tag at the C-terminus of the p66 subunit, was purified to homogeneity by affinity chromatography on a Ni<sup>2+</sup> nitrilotriacetic acid agarose (Ni-NTA) column followed by cation exchange chromatography, as previously described (18). The

expression plasmids, encoding the single RT mutant Y181C and the double mutant L100I/K103N, were a generous gift from S. Hughes of the National Cancer Institute (Frederick, MD). The Y181C mutant of HIV-1 RT was expressed in *Escherichia coli* BL-21, and the L100I/K103N double mutant was expressed in *E. coli* DH5 $\alpha$ . Both RT mutants, as well as wild-type HIV-2 RT, were purified in a manner similar to that of wild-type HIV-1 RT. Wild-type heterodimeric (p68/p54) HIV-2 RT, Tf1 RT, and PERV RT were expressed and purified as previously described (19–21). Taq and Vent polymerases were purchased from New England Biolabs Inc.

**Quantitative Assays for RT Activities.** The RDDP activity of RT was assayed by measuring the level of incorporation of [ $^3$ H]dTTP into the poly(rA) $_n$ •oligo(dT) $_{12-18}$  template•primer, as previously described (22). All reaction mixtures were assayed at 37 °C in a final volume of 100  $\mu$ L that included 1% DMSO. To avoid exposure of RT to high local DMSO concentrations, 1  $\mu$ L of each inhibitor, diluted in concentrated DMSO (or 1  $\mu$ L of DMSO as a control), was added to 79  $\mu$ L of a buffer and the solution mixed, and only then were the rest of the other reaction components, including RT, added. The DDDP activity of RT was assayed in a similar manner but with activated herring sperm DNA at a final concentration of 20  $\mu$ g/mL, substituting for the synthetic template•primer, and with all four dNTPs present in the reaction mixture. Taq and Vent DDDP activity was assayed at 75 °C according to the manufacturer's unit definition.

The RNase H activity was assayed by monitoring the release of [ $^3$ H]AMP-containing fragments from the substrate [ $^3$ H]poly(rA) $_n$ •poly(dT) $_n$  as previously described in detail (23).

All calculated values reported herein are the averages of at least three experiments. The dose–response curves were nonlinearly fitted to the four-parameter logistic equation (24) using GraphPad prism 4 or Origin 7.5.

**Cytotoxicity.** A cytotoxic assay was performed in a 96-well plate using B lymphocytes (721.221 cells) and XTT substrate as previously described (25). Absorbance was recorded at 450 nm, and the reference wavelength was recorded at 630 nm.

**Kinetic RDDP Assays.** Kinetic assays were conducted as described above for the quantitative analysis but with different concentrations of dTTP or poly(rA) $_n$ •oligo(dT) $_{12-18}$  template•primer as indicated. Reaction mixtures were incubated for 12.5 min, and the results were linearly fit according to the specified analysis using GraphPad prism 4 or Origin 7.5.

**DNA-Primer Extension Reactions.** All reactions were performed with single-stranded circular  $\phi$ X174am3 DNA that served as a template and was primed with a synthetic 15-mer oligonucleotide (5'-AAAGCGAGGGTATCC-3'), which hybridizes to positions 588–602 of the template DNA as previously described (26).

**PAGE Mobility Shift Assay.** Formation of a complex of  $^{32}$ P 5'-end-labeled DNA oligonucleotide and HIV-1 RT was detected by the electrophoretic retardation of the DNA as a result of its association with RT, as previously described in detail by us (27). All reaction mixtures included up to 4% DMSO, which did not show any effect on complex formation, as tested in preliminary experiments (data not shown).

**Surface Plasmon Resonance (SPR) Experiments.** All experiments were carried out on a BIACORE 3000 system

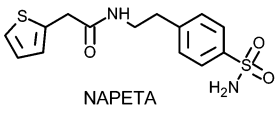
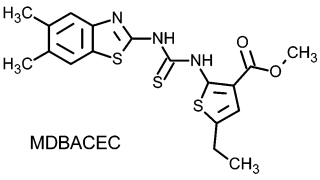
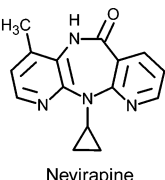
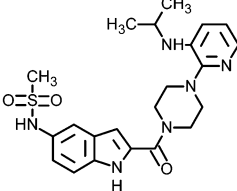
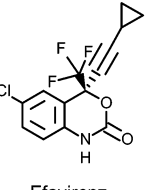
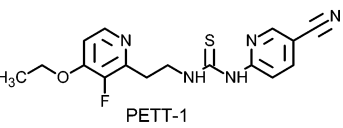
with standard HBS buffer [10 mM HEPES (pH 7.4), 150 mM NaCl, 3.4 mM EDTA, and 0.05% Tween 20]. Immobilization of DNA on a CM5 research grade chip was carried out under a continued flow of HBS at 10  $\mu$ L/min in two steps. First, neutravidin (Pierce) was immobilized on two channels of the chip by injection of 70  $\mu$ L of 0.2 M EDC and 0.05 M NHS, followed by short injections of neutravidin [500  $\mu$ g/mL in 10 mM sodium acetate (pH 4.6)]. The remaining active esters were blocked by injection of 70  $\mu$ L of 1 M ethanolamine. This procedure resulted in a total of ~4500 response units (RU) of neutravidin, immobilized on each of two channels of the chip. Finally, 18  $\mu$ L of 0.8  $\mu$ M biotinylated double-stranded DNA (5'-TGAC-CAAGGGCTAATTCACCT-biotin and 5'-AGTGAATTAGC-CCTTGGTCA-biotin) was injected over one surface of the chip followed by a second injection over the same surface of 20  $\mu$ L of a 1.2  $\mu$ M solution, both at 5  $\mu$ L/min. Loosely attached material was removed by injecting 10  $\mu$ L of 0.05% sodium dodecyl sulfate (SDS). This resulted in one reference surface on which neutravidin was immobilized and one active surface on which the DNA was immobilized through neutravidin. All kinetic experiments of the binding of RT to the immobilized biotinylated DNA were carried out in HBS buffer that included 2% DMSO (and all samples included 2% DMSO as well). The specified RT concentration was mixed with the indicated NAPETA concentration (or with 2% DMSO substituting for the inhibitor) and then injected for 2 min over the chip at a flow rate of 10  $\mu$ L/min. The surface was regenerated with a short pulse of 0.05% SDS (10  $\mu$ L at a flow rate of 20  $\mu$ L/min). For each concentration, the signal recorded from the reference (control) channel was subtracted from the signal recorded from the active channel. The various concentrations were overlaid and then nonlinearly fitted to a simple bimolecular model (RT + DNA = RT•DNA) with minimal adjustments for signal drifting (<0.03 RU per second) using BIAevaluation. For more reliable results, analysis of the interaction of RT with the DNA was fitted with one global value for  $R_{\max}$ . The same  $R_{\max}$  value was used for the same interaction in the presence of the inhibitor.

## RESULTS

**Virtual Screening of a Chemical Library against Wild-Type HIV-1 RT Structures.** To identify novel inhibitors against HIV-1 RT, we virtually screened 50 000 compounds, which are found in the diversity chemical library from Chembridge, against two crystal structures of HIV-1 RT. Each compound was energy minimized with Omega, and the resulting molecular structures were then docked into the heterodimeric structure of RT found in PDB entry 1fk9 (after removal of the bound inhibitor) with Suflex. Each docked molecule was scored according to its calculated binding affinity and whether there were any crashes with RT. To account for subtle differences among the different RT structures and to validate the docking scores, the top scored molecules were then docked into the second structure of RT (PDB entry 1dtq). Compounds that exhibited high affinity for both RT structures were further analyzed by visually inspecting their docked conformation for the quality of the docking process. On the basis of all these steps, a total of 56 compounds that met all criteria were selected and purchased from Chembridge.



Table 1: Structure, Docking Results, and Molecular Properties of Compounds Which Inhibited the RDDP Activity of HIV-1 RT with  $IC_{50}$  Values of  $<10 \mu M$  and Reference NNRTIs

<div style="display: flex; justify-content: space-around; align-items: flex-start;"> <div style="text-align: center;">  <p>NAPETA</p> </div> <div style="text-align: center;">  <p>MDBACEC</p> </div> <div style="text-align: center;">  <p>Nevirapine</p> </div> <div style="text-align: center;">  <p>Delavirdine</p> </div> <div style="text-align: center;">  <p>Efavirenz</p> </div> <div style="text-align: center;">  <p>PETT-1</p> </div> </div>						
	tested compounds		reference molecules			
	NAPETA	MDBACEC	nevirapine	efavirenz	delavirdine	PETT-1
Docking Results						
structure 1fk9						
score <sup>a</sup>	7.07	7.15	5.66	6.51	5.51	7.18
crash <sup>b</sup>	-1.9	-1.01	-1.25	-0.65	-3.79	-1.34
polar <sup>c</sup>	2.34	2.69	0	1.99	1.23	1.7
structure 1dtq						
score <sup>a</sup>	5.74	3.44	4.87	5.11	3.57	7.23
crash <sup>b</sup>	-3.21	-4.04	-1.31	-0.87	-4.91	-1.85
polar <sup>c</sup>	2.86	1.22	0	1.14	0.02	0.81
Molecular Properties						
molecular weight	324.42	405.56	266.3	315.68	456.57	345.40
no. of H-bond donors	2	2	1	1	3	2
no. of H-bond acceptors	4	3	5	3	9	6
Log P	0.59	4.92	1.38	4.53	2.88	2.34
TPSA <sup>d</sup>	89.26	63.25	63.58	38.33	110.43	82.86
no. of rotatable bonds	6	3	1	1	6	8

<sup>a</sup> Score is the estimated affinity [ $-\log(K_d)$ ] of the inhibitor. <sup>b</sup> Crash is a measure of the inappropriate penetration into the protein by the ligand and of internal self-clashing that the ligand is experiencing. A minimum crash value is desirable. When Surflex was evaluated by comparing docking results to crystallographic experimental data, the docked ligands were within 1.5 Å root-mean-square deviations of the crystallized ligands (which is a very accurate docking) in 89% of the protein-ligand pairs. In these cases, a penalty between 0 and -3.2 was reported (16). <sup>c</sup> Polar is the contribution of polar interaction to the total affinity. A perfect hydrogen bond contributes ~1.2 units, whereas a charged interaction contributes up to 2.3 units (16). The desirable value depends on the aim of the screen. Filtering for minimum polar values can be used to identify compounds that interact mostly through hydrophobic bonds. On the other hand, filtering for maximum polar values can be used to identify compounds that interact mainly by hydrogen and charged contacts. <sup>d</sup> Topological polar surface area (square angstroms).

All selected chemicals were tested for in vitro inhibition of the RDDP activity of HIV-1 RT, and two of them inhibited this activity with inhibitor concentrations inhibiting 50% of the initial RT activity ( $IC_{50}$  values) of  $<10 \mu M$  (Table 1). The two compounds, NAPETA and MDBACEC, also exhibited high affinity for RT according to the in silico docking results. Interestingly, higher scores, which reflect tighter binding, were observed against the 1fk9 structure than against the 1dtq structure. Averaging the scores over both RT structures indicated that NAPETA could bind RT more strongly than MDBACEC with scores of 6.4 and 5.3, respectively. This was also supported experimentally, since NAPETA inhibited completely the RT-associated RDDP activity at  $10 \mu M$ , whereas MDBACEC inhibited only 83% of the initial RT activity at the same concentration (data not shown). The docking process was also repeated with four known NNRTIs, which were used as references. Nevirapine, efavirenz, and delavirdine are drugs currently used for anti-HIV therapy, whereas PETT-1 belongs to the PETT NNRTIs that were intensively studied in the past. Overall docking scores were high (Table 1) with average scores over both

RT structures of 5.27, 5.81, 4.54, and 7.2 for nevirapine, efavirenz, delavirdine, and PETT-1, respectively. Nevirapine and efavirenz inhibited the RDDP activity of HIV-1 RT in our experimental system with  $IC_{50}$  values of 1.7  $\mu M$  and 11 nM, respectively. Reported  $IC_{50}$  values of delavirdine and PETT-1 for inhibiting this HIV-1 RT activity were between 0.26–2.18  $\mu M$  in different systems (28–30) and 6 nM, respectively. Accordingly, the apparent inhibition efficiencies of the NNRTIs were in the following order: PETT-1  $\geq$  efavirenz  $>$  nevirapine  $\geq$  delavirdine (which was the same ranked order predicted from their average docking scores). Interestingly, binding affinities of nevirapine, delavirdine, and PETT-1 toward RT were calculated from their docking scores ( $10^{-\text{score}}$ ) as 5.4  $\mu M$ , 29  $\mu M$ , and 63 nM, respectively, and were in close agreement with their experimental  $IC_{50}$  values. The estimated binding affinity of efavirenz was more deviated from its experimental data in comparison with those of the other inhibitors. However, it should also be emphasized that only under certain circumstances does the binding affinity of an inhibitor for an enzyme equal its  $IC_{50}$  value

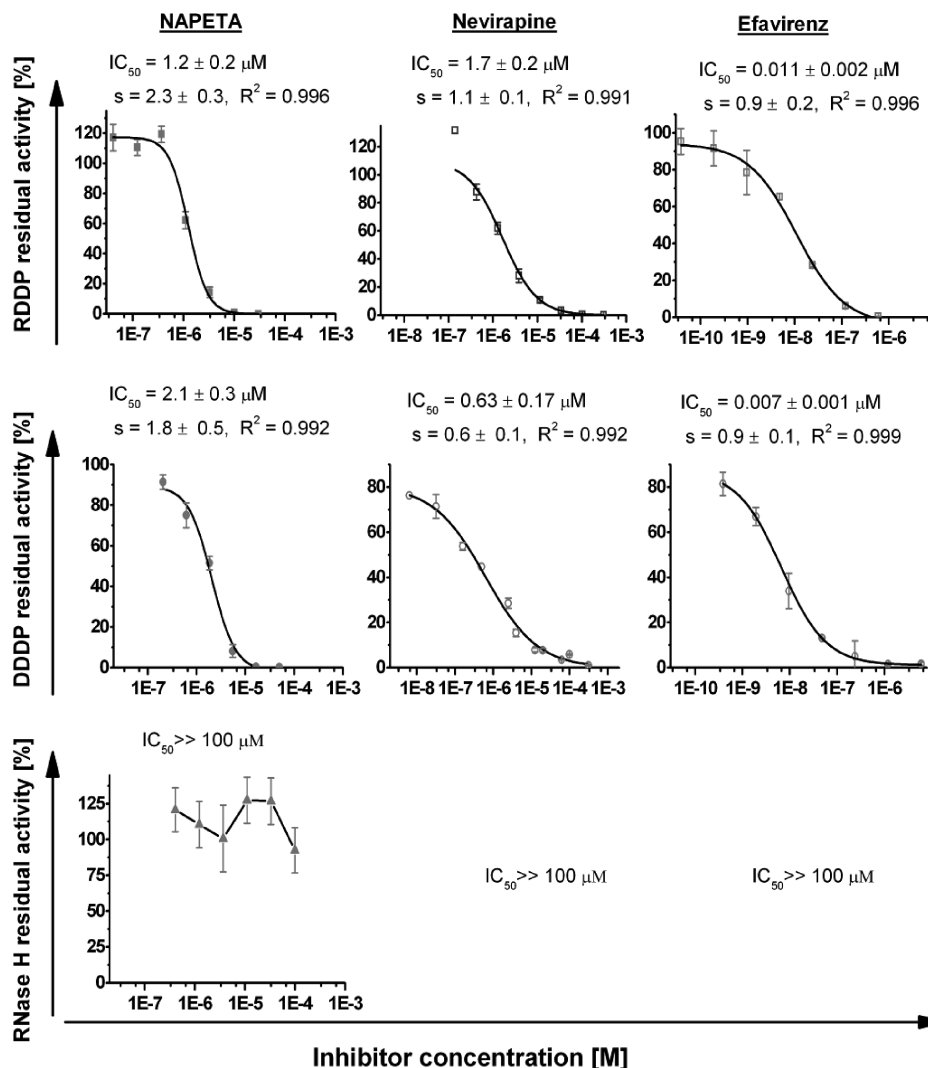


FIGURE 1: Effect of NAPETA, nevirapine, and efavirenz on the enzymatic activities of wild-type HIV-1 RT. RDDP (top), DDDP (middle), and RNase H (bottom) activities were assayed in the presence of increasing inhibitor concentrations. Dose–response curves were fitted to a four-parameter logistic equation, and the apparent  $IC_{50}$  values as well as standard errors and correlation coefficients are indicated.

with out any dependence on substrate concentration. This relationship was demonstrated for noncompetitive inhibition that followed Michaelis–Menten kinetics (31), but it is not necessarily valid for all the four tested inhibitors. Similar to most NNRTIs, NAPETA has a low molecular weight and does not violate any of the Lipinski rule of 5, which uses molecular properties to predict absorption and permeation capabilities [more than five H-bond donors, 10 H-bond acceptors, a molecular weight greater than 500, and a calculated Log P greater than 5 are likely to result in poor absorption or permeation (32)]. Therefore, it was further evaluated.

**Inhibition of HIV-1 RT Activity.** NAPETA was tested against all HIV-1 RT activities, specifically, RDDP, DDDP, and RNase H. For each activity, the  $IC_{50}$  values were calculated from dose–response curves using increasing concentrations of the inhibitor (Figure 1). NAPETA inhibited the RDDP activity with an apparent  $IC_{50}$  value of  $1.2 \mu M$  and the DDDP activity with an  $IC_{50}$  of  $\sim 2.1 \mu M$ . In contrast, this inhibitor did not inhibit the RNase H activity, showing that NAPETA is specific against the DNA polymerase activity. The inhibition of HIV-1 RT by NAPETA was also compared to those of two clinically used NNRTIs under

identical experimental conditions (Figure 1). Nevirapine inhibited HIV-1 RT with  $IC_{50}$  values of  $\sim 1.7 \mu M$  for the RDDP activity and  $0.63 \mu M$  for the DDDP activity; both were comparable to the inhibition by NAPETA. Efavirenz was more potent and inhibited RDDP RT activity with an  $IC_{50}$  value of 11 nM and DDDP RT activity with an  $IC_{50}$  value of 7 nM. As expected, both inhibitors did not inhibit the RNase H activity of HIV-1 RT. Interestingly, both nevirapine and efavirenz exhibited a sigmoid factor close to 1 in both assays. This was in contrast to NAPETA in which the sigmoid factor of the fitted curves was calculated to be close to 2 in both DNA polymerase assays. This indicates that the HIV-1 RT molecule may have two different binding sites for NAPETA and that the mechanism of action of this drug is probably different from the mode of action of the other two clinically used NNRTIs.

**Effects of NAPETA on HIV-1 RT Drug-Resistant Variants and on Other DNA Polymerases.** To further evaluate the potency of the inhibitor, NAPETA was also tested for inhibiting two drug-resistant mutants of HIV-1 RT as well as wild-type HIV-2 RT and several other DNA polymerases. NAPETA inhibited efficiently the RDDP activity of the Y181C mutant of HIV-1 RT with an  $IC_{50}$  value of  $7.4 \mu M$

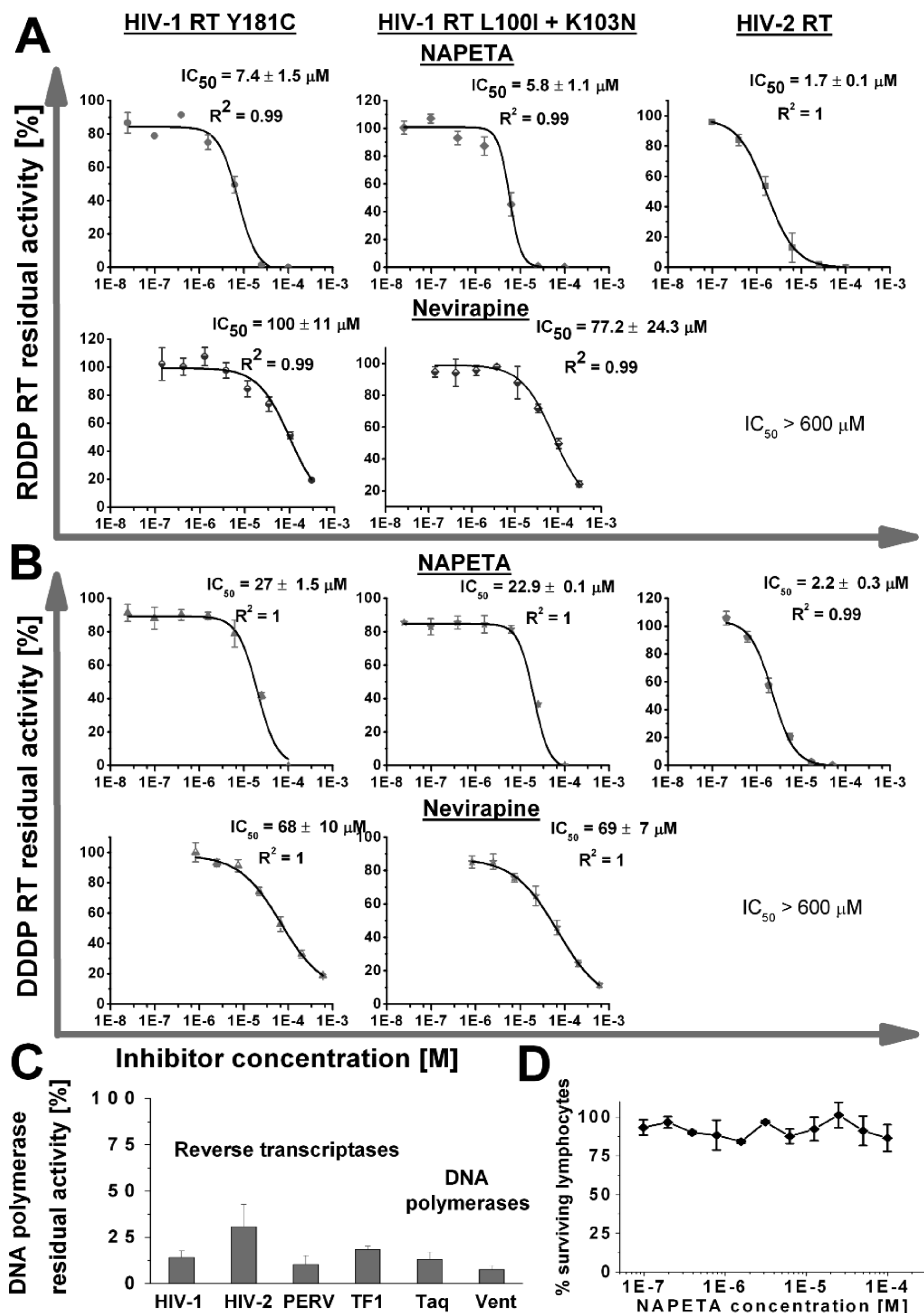


FIGURE 2: Effects of NAPETA on two drug-resistant HIV-1 RT variants, wild-type HIV-2 RT, and different DNA polymerases. RDDP (A) and DDDP (B) activities of the two HIV-1 RT mutants (Y181C and L100I/K103N) and of wild-type HIV-2 RT were assayed in the presence of various concentrations of NAPETA or nevirapine as specified. The measured dose-response curves were fitted to the logistic equation, and the  $IC_{50}$  values along with the associated standard error, sigmoid factor, and correlation coefficient are reported. The reference results for the inhibition of RDDP activity of the two mutants by nevirapine were taken from our previous study published recently. Reproduced with permission from ref. 34. Copyright 1998 American Chemical Society. Reported values are the averages of assays conducted in triplicate. (C) Effects of a single dose of  $3.3 \mu M$  NAPETA on the DNA polymerase activity of different enzymes. This concentration corresponds to the first minor tick after  $1E-6$  M on the X-axis of each graph in this figure and in Figure 1 for comparison. Residual activity of HIV-1 RT was taken from Figure 1 (NAPETA), and all other residual activity values were calculated from other independent experiments. All RTs were assayed for their RDDP activity, whereas Taq and Vent polymerase were assayed for their DDDP activity. (D) Effect of NAPETA on the viability of lymphocytes. Results are presented as the percentage of surviving cells based on the absorbance measured for cells incubated in the absence of NAPETA. Each NAPETA concentration was tested in a triplicate.

and the K103N/L100I double mutant with an  $IC_{50}$  value of  $5.8 \mu M$  (Figure 2A). Inhibition of the DDDP activity of the mutant RTs was also evaluated. In comparison to wild-type HIV-1 RT, NAPETA was 12.3-fold less effective against Y181C RT and 10.4-fold less effective against the double mutant RT (Figure 2B). The comparison of this inhibition capacity for nevirapine, which was used as reference, showed that NAPETA inhibited both DNA polymerase activities of the two drug-resistant mutants of HIV-1 RT substantially more effectively than nevirapine did (Figure 2A,B). Interest-

ingly, the efficiency of HIV-2 RT inhibition was similar to that of HIV-1 RT, as the  $IC_{50}$  values determined for the inhibition of both HIV-2 RT-associated activities were  $\sim 2 \mu M$  (Figure 2A,B). Such ability was not exhibited by nevirapine, which did not inhibit at all HIV-2 RT over the range of tested concentrations (Figure 2A,B). Further analysis showed that NAPETA could inhibit other RTs such as those of PERV, MLV, and even bacterial Taq and archaeobacterial Vent DNA polymerases, indicating that it may have several modes of binding and at least one of them may be directed

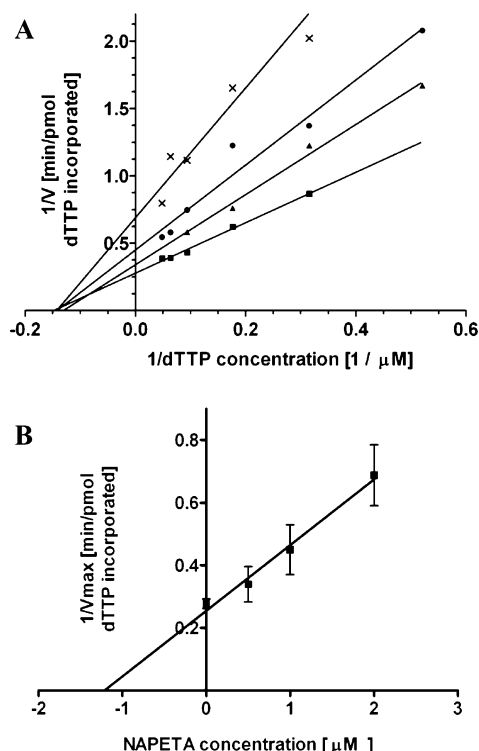


FIGURE 3: Kinetic analysis of the inhibition of HIV-1 RT-associated DNA polymerase activity by NAPETA with respect to dTTP substrate. (A) Double-reciprocal plot of the initial velocity of the RDDP activity of HIV-1 RT as a function of dTTP substrate concentration. Increasing concentrations of dTTP in the absence (■) or presence of 0.5 (▲), 1 (●), or 2  $\mu M$  NAPETA (×). (B) Replot (Dixon) of the reciprocal maximal velocity (calculated from panel A) vs various NAPETA concentrations. The kinetic constants  $K_m$  and  $K_i$  were calculated after linear regression analysis.

against a conserved site which is shared by all tested DNA polymerases (Figure 2C). Most importantly, NAPETA inhibited a wide range of DNA polymerases without causing any significant cytotoxic effects on B lymphocytes for concentrations up to 100  $\mu M$  (Figure 2D), which is much higher than its effective inhibition concentration. As NAPETA did not inhibit the RT-associated RNase H activity, we conclude that its inhibition is specific to the DNA polymerase activity.

**Kinetic Analysis of the Inhibition of Wild-Type HIV-1 RT and HIV-2 RT by NAPETA.** Steady state kinetic studies were performed by assaying the RDDP activity of wild-type HIV-1 RT in the presence of increasing concentration of each substrate and a specific NAPETA concentration. These assays were repeated with a range of NAPETA concentrations, and the results were analyzed by double-reciprocal (Lineweaver–Burk) plots. RT inhibition with respect to the dTTP substrate showed a classical noncompetitive behavior with no significant change in the apparent  $K_m$  values in the presence of NAPETA (Figure 3). The control value for the reaction without inhibitor was  $\sim 6.8 \mu M$  dTTP, whereas the average  $K_m$  values in the presence of 0.5, 1, and 2  $\mu M$  NAPETA were  $7.3 \pm 0.4 \mu M$ . In accordance with this mode of inhibition, the  $K_{cat}$  values ( $V_{max}/[RT]$ ) were decreased by the compound from approximately  $0.6 s^{-1}$  in the absence of inhibitor to 0.5, 0.37, and  $0.25 s^{-1}$  in the presence of 0.5, 1, and 2  $\mu M$  NAPETA, respectively. Thus, it is likely that dTTP and the inhibitor could bind RT independently. A replot of

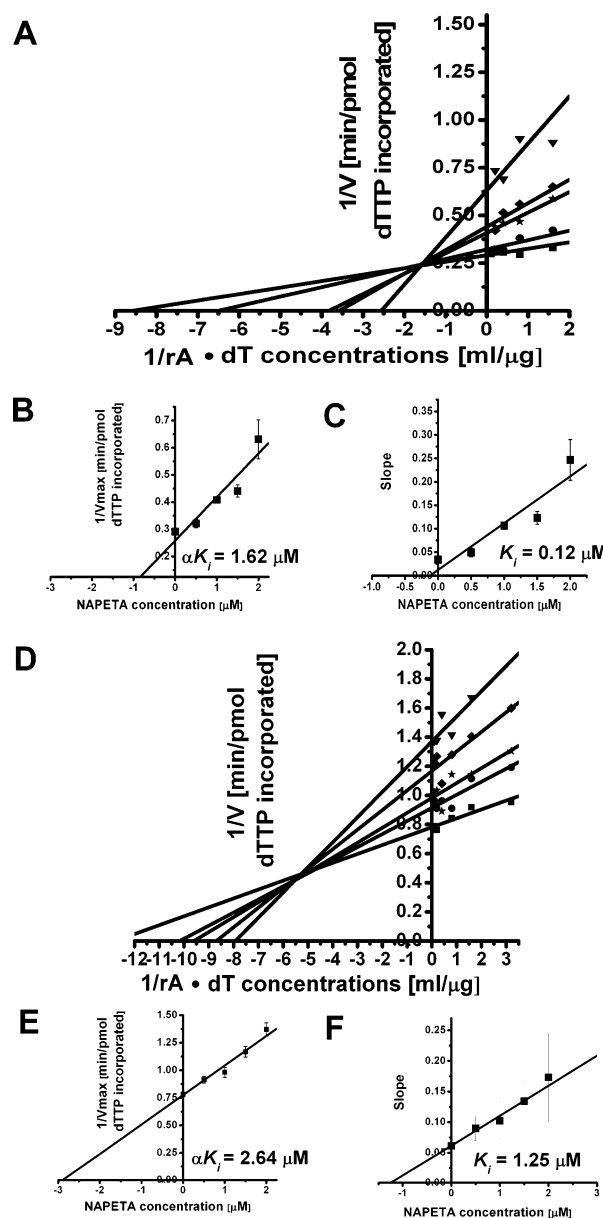


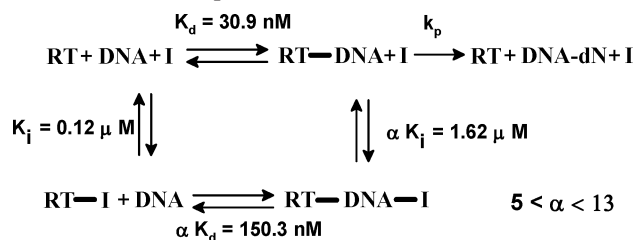
FIGURE 4: Kinetic analysis of the inhibition of HIV-1 and HIV-2 RT-associated DNA polymerase activities by NAPETA with respect to the rA·dT substrate. (A) Double-reciprocal plot of the initial velocity of RDDP activity of HIV-1 RT as a function of poly(rA)<sub>n</sub>·oligo(dT)<sub>12–18</sub> substrate concentration. Increasing concentrations of the substrate in the absence (■) or presence of 0.5 (●), 1 (★), 1.5 (◆), or 2  $\mu M$  NAPETA (▼). (B) Replot (Dixon) of the reciprocal maximal velocity (calculated from panel A) vs various NAPETA concentrations. (C) Replot of the slope (calculated from panel A) vs various NAPETA concentrations. The kinetic constants  $K_i$  and  $\alpha K_i$  were calculated by linear regression analysis. Panels D–F are the equivalents of panels A–C, respectively, performed with wild-type HIV-2 RT.

$1/V_{max}$  values against the inhibitor concentrations (Dixon plot) was linear with a correlation coefficient ( $r^2$ ) of 0.99 and yielded a  $K_i$  value of  $\sim 1.2 \mu M$  (Figure 3B).

Inhibition of RT with respect to the template·primer (rA·dT) was more complex and showed a mixed-linear pattern. According to the double-reciprocal plot, NAPETA was capable of simultaneously lowering the  $V_{max}$  and increasing the  $K_m$  values of the reaction, and both effects were dose-dependent (Figure 4). NAPETA suppressed the  $V_{max}$  values from  $\sim 3.4$  pmol of dTTP/min (with no inhibitor) to ap-



Scheme 1: Proposed Model for the Inhibition of HIV-1 RT-Associated DNA Polymerase Activity with Respect to the RNA•DNA Template



proximately 3.1, 2.5, 2.3, and 1.6 pmol of dTTP/min using 0.5, 1, 1.5, and 2  $\mu\text{M}$  inhibitor, respectively. At the same time, the compound led to an increase in  $K_m$  from  $\sim 0.12 \mu\text{g/mL}$  (with no inhibitor) to approximately 0.15, 0.26, 0.28, and 0.39  $\mu\text{g/mL}$  rA•dT, obtained at those identical NAPETA concentrations, respectively. This apparent mode of inhibition was fitted to a mixed-linear type of inhibition and was characterized by an  $\alpha$  factor, which modifies both the binding of the inhibitor to the RT•template•primer complex and the binding of the template•primer to the RT•inhibitor complex. Application of this model (Scheme 1) to the data enabled us to calculate the  $K_i$  and  $\alpha K_i$  values from replots of the original reciprocal plot (Figure 4A). A replot of NAPETA concentrations versus the  $1/V_{\max}$  values, associated with each concentration, was used to calculate  $\alpha K_i$  (from the X-intercept), resulting in a value of  $\sim 1.62 \mu\text{M}$ , with a relatively high correlation coefficient ( $r^2$ ) of 0.9 (Figure 4B). A second replot of NAPETA concentrations versus the slope associated with each substrate concentration was used to calculate  $K_i$  (from the X-intercept), resulting in a value of  $\sim 0.12 \mu\text{M}$ , with a correlation coefficient ( $r^2$ ) of 0.9 (Figure 4C). Using these two values, the  $\alpha$  factor was calculated ( $\alpha K_i/K_i$ ) to be 13.5.

The same complex pattern of inhibition with respect to the template•primer (rA•dT) was also demonstrated for the inhibition of HIV-2 RT after the exact kinetic experiment was repeated with this enzyme (Figure 4D–F). In this case, NAPETA suppressed the  $V_{\max}$  value from  $\sim 1.3$  pmol of dTTP/min (with no inhibitor) to approximately 1.1, 1, 0.9, and 0.7 pmol of dTTP/min, using 0.5, 1, 1.5, and 2  $\mu\text{M}$  inhibitor, respectively. At the same time, the compound led to an increase in  $K_m$  from  $\sim 0.080 \mu\text{g/mL}$  (with no inhibitor) to approximately 0.098, 0.104, 0.115, and 0.126  $\mu\text{g/mL}$  rA•dT, obtained at those identical NAPETA concentrations, respectively. Replotting NAPETA concentrations either versus the calculated  $1/V_{\max}$  values (Figure 4E) or against the slope values associated with each substrate concentration (Figure 4F) showed a high correlation coefficient ( $r^2$ ) of 0.97 or 0.98, respectively. On the basis of these plots, the  $\alpha K_i$  value was calculated to be  $2.64 \mu\text{M}$ , whereas the  $K_i$  value was calculated to be  $1.25 \mu\text{M}$ , resulting in an  $\alpha$  factor of  $\sim 2.11$ .

**Reversibility of HIV-1 RT Inhibition by NAPETA.** Both noncompetitive and mixed-linear inhibitions rely on the reversibility of the inhibitor binding to RT. To verify this type of binding, NAPETA was tested with increasing RT concentrations at saturating concentrations of both dTTP and rA•dT (Figure 5). As expected, plotting the RT concentration against its apparent  $V_{\max}$  values obtained in the absence or presence of 1.5  $\mu\text{M}$  inhibitor showed intercepting rather than

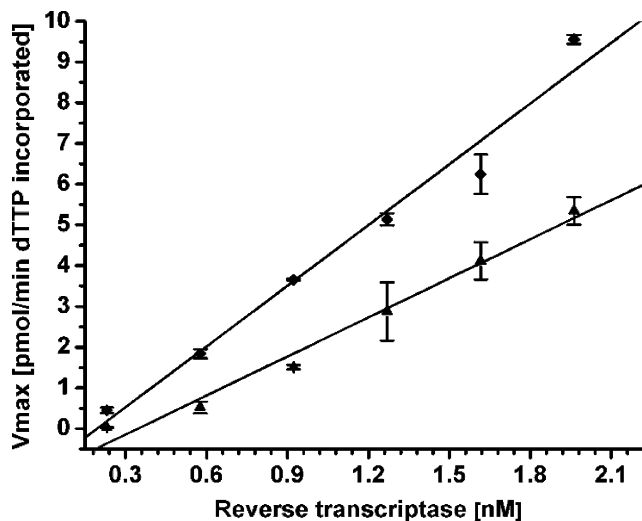


FIGURE 5: Maximal velocity of HIV-1 RT-associated DNA polymerase activity as a function of enzyme concentration. The DNA polymerase activity was monitored by assessing the poly-(rA)<sub>n</sub>•oligo(dT)<sub>12–18</sub>-directed incorporation of [<sup>3</sup>H]dTTP into DNA in the absence (◆) or presence of 1.5  $\mu\text{M}$  NAPETA (▲). The reactions were performed with saturating concentrations of dTTP (15  $\mu\text{M}$ ) and template•primer (8.5  $\mu\text{g/mL}$ ) for 15 min at 37 °C. The curves were fitted by linear regression analysis that resulted in high correlation coefficients ( $r^2$ ) of 0.97 (without inhibitor) and 0.99 (with inhibitor), indicating a strong linear relationship between  $V_{\max}$  values and enzyme concentrations.

parallel lines. In other words, the RT activity in the presence of NAPETA was proportionally increased as a function of RT concentration with  $51 \pm 12\%$  inhibition of the activity at all tested RT concentrations (excluding the lower RT concentration that showed stronger inhibition, probably due to a significantly higher ratio of inhibitor to RT). This excluded the possibility that a fraction of RT was irreversibly eliminated by the inhibitor and suggested reversible binding between RT and NAPETA.

**Inhibition of DNA-Primer Extension of Wild-Type HIV-1 RT.** To gain better insights into the mechanism by which NAPETA inhibits RT, we have followed the extension of a 5'-end-labeled 15-mer DNA primer, annealed to  $\phi\text{X174}$  single-stranded DNA, in the presence of a high inhibitor concentration. The overall primer extension without any inhibitor resulted in the production of DNA molecules up to  $\sim 500$ -mer in length. To test whether NAPETA could bind to the RT•DNA complex, we have also alternated the order of addition of the template•primer and the inhibitor. The inhibitor showed complete inhibition of primer extension when it was first incubated with RT prior to substrate DNA (lane 3). This pattern remained unchanged when we first incubated RT with the template•primer and then added the inhibitor (lane 7). This means that the ability of NAPETA to bind RT after the formation of the RT•DNA complex was preserved. The same pattern of inhibition was also observed with nevirapine and efavirenz, at concentrations similar to that of NAPETA, that were used as a positive classical NNRTIs controls (lanes 4, 5, 8, and 9).

**Effect of NAPETA on the Binding of HIV-1 RT to DNA.** The formation of the RT•DNA complex can be monitored by a gel shift assay, in which an electrophoretic retardation of radiolabeled DNA is detected as a result of its association with RT. Performing this assay in the presence of the



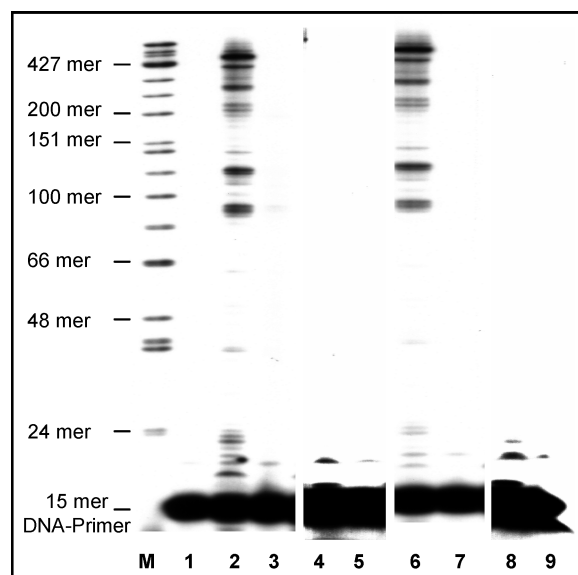


**FIGURE 6:** Effects of NAPETA on DNA primer extension by HIV-1 RT. Primer extension reactions were carried out as described in Experimental Procedures. The DNA products of the extended  $^{32}\text{P}$ -end-labeled 15-mer oligonucleotide annealed to single-stranded  $\phi\text{X174am3}$  DNA were analyzed by urea-PAGE. Molecular size markers were  $\text{HinfI}$ -cleaved double-stranded dephosphorylated  $\phi\text{X174}$  DNAs that were 5'-end-labeled with  $[\gamma\text{-}^{32}\text{P}]\text{ATP}$ . In all reactions (except for the control), 4.7 nM HIV-1 RT was preincubated on ice for 30 min. Lane m contained markers, and lane 1 was the control with no enzyme. In lanes 2–5, RT was preincubated with DMSO, 500  $\mu\text{M}$  NAPETA, 500  $\mu\text{M}$  nevirapine, and 500  $\mu\text{M}$  efavirenz, respectively, followed by the addition of the template-primer (T/P). In lanes 6–9, RT was preincubated with T/P followed by addition of DMSO, 500  $\mu\text{M}$  NAPETA, 500  $\mu\text{M}$  nevirapine, and 500  $\mu\text{M}$  efavirenz, respectively. The reactions were initiated with the addition of the relevant substrates, and the mixtures were further incubated at 37 °C for 25 min. All reaction mixtures included a final DMSO concentration of 2%.

inhibitor showed that the association of RT with DNA was impaired by NAPETA in a dose-response manner (Figure 7A). The complex formation is notable in lane 2, where no inhibitor was present. In contrast, the quantity of this complex is substantially decreased in lanes 3–5, where RT was assayed in the presence of 500, 720, and 1000  $\mu\text{M}$  NAPETA, respectively. High NAPETA concentrations were required to observe this effect, since, in order to achieve substantial complex formation, the assay required RT concentrations that were 130-fold higher than those used in the DNA polymerase assays (described above for calculating the  $\text{IC}_{50}$  values). Therefore, it is reasonable that an  $\sim 150$ -fold higher concentration of NAPETA was required to obtain the same inhibitor/RT ratio. To verify that migration of the DNA was not affected by NAPETA, we have performed the same experiment without RT (Figure 7B, lanes 3 and 4). As expected, the presence of NAPETA by itself did not modify the DNA migration pattern. The ability of NAPETA to affect the binding of RT to DNA was not unique to this inhibitor as it was also seen with other RT inhibitors, such as inhibitory peptides (33). In contrast to this pattern, two clinically used drugs, nevirapine and efavirenz, which were used as controls, induced a stronger binding of RT to its DNA template than the binding without inhibitor (Figure 7B, lanes 5, 6, 9, and 10). This evidence, once again, supports the unique nature of NAPETA in comparison to other NNRTIs. As expected, neither nevirapine nor efavirenz by

itself affected the DNA migration (Figure 7B, lanes 7, 8, 11, and 12).

The interference of NAPETA with the binding of RT to DNA was further quantified, using a SPR technology (BIACORE 3000). The technology monitors bimolecular interactions directly in real time (with no intermediates involved), using a noninvasive optical detection principle. The SPR response reflects changes in mass concentrations at the detector surface, as molecules bind or dissociate. One of the interactants is immobilized on a surface, while the other is injected into a continuous flow over the surface. Biotinylated double-stranded short synthetic DNA was immobilized onto a dextran chip through neutravidin followed by the injection of RT over the chip in the absence or presence of the inhibitor. Injection of wild-type HIV-1 RT at a final concentration of 235 nM resulted in a signal that reached  $\sim 115$  RU, while injections of the same RT concentration with increasing NAPETA concentrations resulted in a substantially reduced signal (Figure 8a). NAPETA (500  $\mu\text{M}$ ) abolished completely the binding of RT to DNA in this assay, which seems, therefore, more sensitive to effects of NAPETA than the gel shift assay (Figure 7). The kinetics of RT-DNA binding were then monitored by injecting various concentrations of RT over the chip. In the absence of inhibitor, the resulting signal was concentration-dependent and could be fitted to a simple bimolecular interaction with low  $\chi^2$  of 2.8 and a good match between the suggested model and the experimental data (Figure 8b). The apparent association and dissociation rate constants were calculated to be  $\sim 2.9 \times 10^5 \text{ M}^{-1} \text{ s}^{-1}$  and  $\sim 8.9 \times 10^{-3} \text{ s}^{-1}$ , respectively. The same analysis in the presence of NAPETA showed a marked decrease in the intensity of the signal, with association and dissociation rate constants of  $\sim 0.63 \times 10^5 \text{ M}^{-1} \text{ s}^{-1}$  and  $\sim 9.47 \times 10^{-3} \text{ s}^{-1}$ , respectively. Calculation of the dissociation equilibrium constant ( $K_d = k_d/k_a$ ) showed that the inhibitor lowered the affinity of RT for DNA by  $\sim 5$ -fold, from  $\sim 31$  to  $\sim 150$  nM. This interference of NAPETA with the formation of the RT-DNA complex further supports the mixed-linear inhibition mechanism observed in the kinetic analyses for NAPETA (see Figure 4), where the affinity constant between RT and the DNA is presumed to be modified by the inhibitor as part of the inhibition. These results also support the gel shift data presented in Figure 7.

## DISCUSSION

In this work, we describe the identification and characterization of a novel potent inhibitor against the DNA polymerase activity of HIV-1 RT. We used molecular modeling to analyze two different structures of RT, in such a way that only molecules docked with high scores into both structures were further tested in vitro for their biochemical effects on the RT-associated enzymatic activities. This novel strategy, which has been successfully used by us against HIV-1 RT mutant structures (34), ensured docking results more reliable than those obtained from a single structure. As it takes into account subtle differences between the two studied RT structures, it may reflect the different experimental conditions employed while crystallizing these protein complexes. In addition, it is well-known that RT binds a wide diversity of molecules, partially because the NNRTI binding pocket is elastic and can be induced to fit specific inhibitors (3). Using two RT structures is expected to result

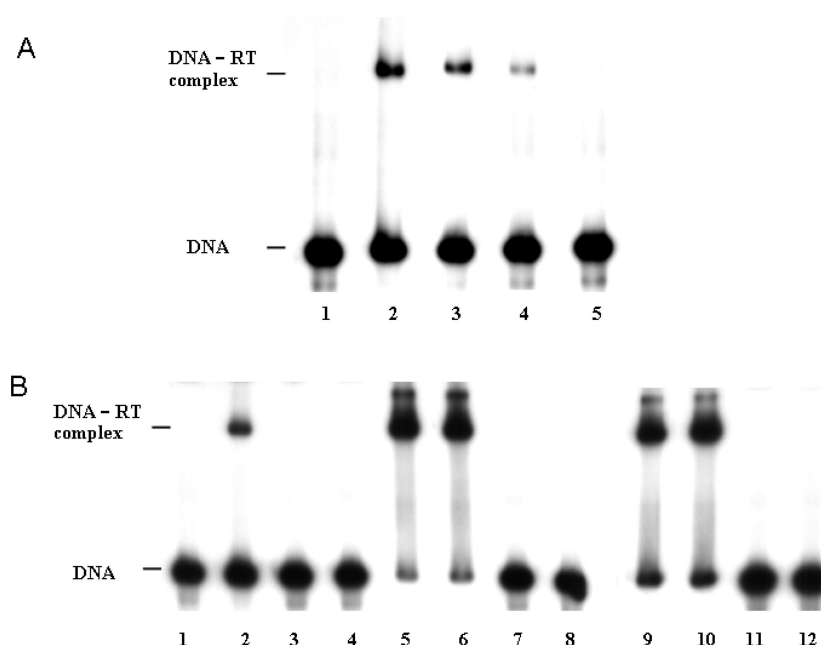


FIGURE 7: Effect of NAPETA on the formation of HIV-1 RT·DNA complexes. The binding of HIV-1 RT to  $^{32}\text{P}$ -end-labeled double-stranded oligonucleotide DNA (54-mer) was carried out in the absence or presence of increasing concentrations of inhibitor as described in Experimental Procedures. The lanes in the scanned autoradiogram of the electrophoretic mobility shift assays are as follows: (A) lane 1, control with no enzyme present; lane 2, binding of RT to DNA with no inhibitor; lanes 3–5, binding of RT to DNA in the presence of 500, 720, and 1000  $\mu\text{M}$  NAPETA (final concentrations), respectively; (B, controls) lane 1, control with no enzyme present; lane 2, binding of RT to DNA with no inhibitor; lanes 3 and 4, mixtures without RT in the presence of final concentrations of 1000 and 500  $\mu\text{M}$  NAPETA, respectively; lanes 5 and 6, binding of RT to DNA in the presence of 1000 and 500  $\mu\text{M}$  nevirapine, respectively; lanes 7 and 8, mixtures without RT in the presence of 1000 and 500  $\mu\text{M}$  nevirapine, respectively; lanes 9 and 10, binding of RT to DNA in the presence of 1000 and 500  $\mu\text{M}$  efavirenz (final concentrations), respectively; lanes 11 and 12, mixtures without RT in the presence of 1000 and 500  $\mu\text{M}$  efavirenz, respectively.

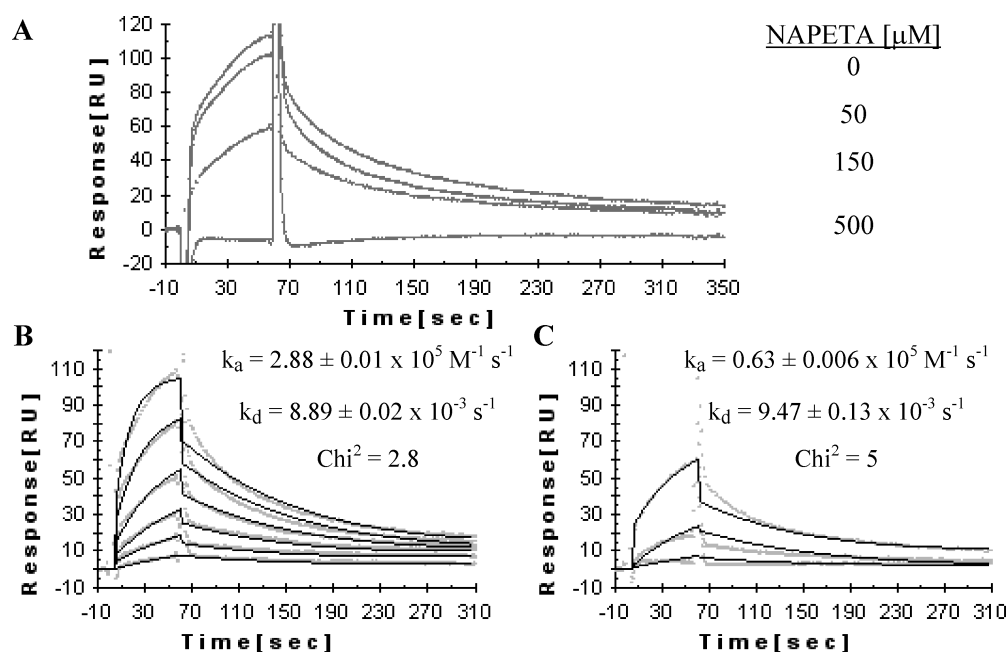


FIGURE 8: Kinetic analysis of the interfering effect of NAPETA on the formation of RT·DNA complexes. The effect of different concentrations of NAPETA on the formation of the RT·DNA complex was monitored by injecting 235 nM RT in the presence of the specified concentrations of NAPETA over a CM5 dextran chip on which biotinylated DNA was immobilized (A). The association and dissociation rate constants between RT and DNA were calculated by injecting RT at final concentrations of 235, 117.5, 59.2, 29.6, 14.8, and 7.4 nM over the chip and fitting the responses to a simple bimolecular interaction (B). The same analysis was done in the presence of 150  $\mu\text{M}$  NAPETA (C). Only top concentrations with a response above baseline were tested and are shown. All analyses were conducted with Biaevaluation and showed  $\chi^2 < 10$  and a good match to the suggested model.

in detection of molecules that can bind the side chain conformations shared by these two structures. The experimental results showed that 3.6% of the compounds tested herein (2 of 56) inhibited efficiently the wild-type HIV-1

RT-associated DNA polymerase activity, which is by far a higher hit rate than that from conventional high-throughput screening (35). NAPETA was the most potent of the two compounds found here, inhibiting specifically the DNA

polymerase activity with no significant effect on the RNase H activity of HIV-1 RT.

NAPETA was also assayed against two drug-resistant variants of HIV-1 RT. Although NAPETA inhibited these two mutants efficiently, the inhibition was slightly less efficient in comparison to the inhibition of wild-type RT. Nevertheless, this compound could still inhibit these mutants more efficiently than nevirapine (Figure 2A,B). Interestingly, unlike classical NNRTIs, NAPETA is also a strong inhibitor of HIV-2 RT and other DNA polymerases (Figure 2), indicating a broad spectrum of inhibition activity without any significant effect on lymphocyte viability. This feature is likely to impose a very high barrier for HIV-1 RT in the development of resistance to NAPETA. The compound showed a slight preference for inhibiting the RDDP activity rather than the DDDP activity of wild-type HIV-1 RT as well as its two mutants tested herein, while these two polymerase activities of wild-type HIV-2 RTs were equally sensitive to NAPETA inhibition. This phenomenon might reflect subtle differences in the interactions of these RTs with the different template·primers that were tested.

Most potent NNRTIs inhibit HIV in cell-based assays at low nanomolar concentrations. For some of them, such as efavirenz and PTT-1, their high inhibition efficacy is evident also in the inhibition of recombinant RT. Other compounds, such as nevirapine and delavirdine, inhibit the recombinant RT with a moderate  $IC_{50}$  in the low micromolar range but still inhibit HIV infection in the nanomolar range. Obviously, in this case, the cell-based assay is more sensitive to inhibition. In addition, other factors, such as membrane permeability, compound stability, and inactivation may influence the extent of inhibition. Accordingly, the efficacy of NAPETA in inhibiting HIV infection requires that it accumulate inside cells up to its effective concentration, which would be higher for HIV carrying the Y181C RT or the double mutant RT than for wild-type HIV. Evidently, NAPETA inhibited recombinant RT in the low micromolar range. The accumulation rate of this compound inside cells along with its outcome on HIV infection can only be evaluated in further detailed experiments that we plan to perform in the future.

Inhibition of the RDDP activity with respect to the dTTP substrate followed a simple noncompetitive inhibition pattern with an apparent  $K_i$  value of  $\sim 1.2 \mu M$ , which matched in this specific case the  $IC_{50}$  value calculated for this activity (Figures 1 and 3). The inhibition of RDDP activity with respect to the RNA·DNA template·primer is apparently more complex, and various approaches were used to elucidate the underlying mechanism. Steady state kinetic analysis (Figure 4) showed that the type of inhibition was a mixed-linear one (as described in Scheme 1), where the inhibitor could bind the free RT (forming RT–I) or the RT-DNA complex (forming RT-DNA–I). In both complex forms, the enzyme is inactive, while the two formed complexes are in continuous equilibration with an equilibrium constant of  $\alpha K_d$ . Only when RT is bound exclusively to the RNA·DNA substrate can it elongate the primer. Interestingly, a similar mode of inhibition was also seen with the inhibition of HIV-2 RT (Figures 2 and 4). A  $K_i$  value of  $1.25 \mu M$  observed for inhibition of HIV-2 RT was higher than the  $K_i$  of  $0.12 \mu M$  observed for HIV-1 RT. In contrast, the  $\alpha$  factor was  $\sim 2$  for HIV-2 RT which was lower than the value of  $\sim 13.5$  measured for

HIV-1 RT. Since the  $\alpha$  factor measures the extent of lowering the affinity of RT for DNA (Scheme 1), it is likely that by binding NAPETA, the capacity of HIV-1 RT to bind DNA is impaired more than the binding of DNA to HIV-2 RT as a result of interacting with NAPETA.

The path from RT-DNA + I to RT-DNA–I in the inhibition model of HIV-1 RT was further supported by the primer extension experiment (Figure 6). We have concluded that the inhibitor is likely to bind the RT-DNA complex, since preincubation of RT with DNA followed by the addition of inhibitor did not alter the extent of inhibition in comparison with the same reaction in which the order of addition was reversed. This ability of NAPETA to inhibit the RT-associated DNA polymerase suggests that all four states of the reaction (RT + DNA + I, RT–I + DNA, RT-DNA + I, and RT-DNA–I) are in a dynamic equilibrium (Scheme 1). In other words, adding the same amount of constituents to the reaction mixture (even in a different order) would result in the same equilibrium in time, since all reactions are reversible, except for the formation of the product. To confirm the model presented in Scheme 1, we have shown that NAPETA can modify the equilibrium constant for binding of RT to DNA by utilizing a gel mobility shift assay (Figure 7). As expected, NAPETA could interfere with the binding of RT to DNA. Moreover, at high concentrations, the inhibitor could completely prevent formation of the RT-DNA complex. In other words,  $\alpha K_d > K_d$  or the inhibitor lowers the affinity of RT for DNA, once it bound RT. This is in accordance with the suggested model, where by definition  $1 < \alpha < \infty$ .

Kinetic studies of the interaction of RT with DNA were further carried out using a SPR analysis. The association rate constant of this complex was diminished by NAPETA from  $2.9 \times 10^5$  to  $0.63 \times 10^5 M^{-1} s^{-1}$ , while the dissociation rate constant was slightly increased from  $8.9 \times 10^{-3}$  to  $9.5 \times 10^{-3} s^{-1}$ . Hence, it is clear that the effect of the inhibitor on the association was more profound than the effect on the dissociation. The association rate constant was suppressed by 5-fold relative to the initial value without inhibitor, while the dissociation rate constant was practically unchanged. On the basis of the SPR assay, the equilibrium constant for formation of the RT-DNA complex was calculated to be  $\sim 31$  nM. This was further confirmed using a modified ELISA-based experiment, where RT at different concentrations was incubated with a biotinylated immobilized DNA and the affinity constant was calculated to be 12 nM (data not shown). These  $K_d$  values were 10-fold (for the SPR experiment) and 4-fold (for the ELISA experiment) higher than the value of 3 nM calculated with a radiolabeled assay for the binding of RT to DNA, as previously reported (12). These differences in the apparent  $K_d$  values could be attributed to different experimental conditions, to different DNA concentrations, or to different active RT concentrations.

On the basis of all the evidence presented here, we conclude that NAPETA inhibited RT by lowering its affinity for the RNA·DNA template. Interestingly, several other compounds were reported to share similar mechanisms of inhibition. KM-1 was found to lower the affinity of RT for DNA in the same manner as NAPETA (12), whereas 2GP is a competitive inhibitor with respect to the template·primer (36). Like NAPETA, the two compounds inhibited drug-resistant RT mutants. KM-1 inhibited several single mutants,



including Y181L, L100I, and K103N, while 2GP inhibited RT that contained five mutations, including Y181C. Evidently, interfering with binding to the RNA·DNA template may target several different mechanisms for the development of resistance by mutant RTs, as 2GP also blocked the excision of AZT-5'-monophosphate from the terminated primer by an AZT-resistant mutant HIV-1 RT. This may enable the compound to overcome the dominant mechanism associated with resistance of HIV-1 RT to AZT inhibition.

NAPETA was shown to inhibit HIV-1 RT with a sigmoid factor close to 2 (Figure 1) and inhibited, as well, several other DNA polymerases. Therefore, we cannot exclude the possibility that NAPETA may bind more than one site of RT. According to this option, one of the interacting sites may be a highly conserved one, common to several DNA polymerases, which is probably different from the hydrophobic pocket against which NAPETA was designed. The second site would probably be the hydrophobic pocket, to which most classic NNRTIs bind.

In summary, the inhibition of RT activity or binding of RT to DNA by NAPETA was demonstrated in several experimental systems. On the basis of the results shown here, a mixed-linear type of inhibition by NAPETA with regard to the RNA·DNA template is suggested by us. As far as we know, NAPETA is a novel molecule and is not found in the anti-HIV compound database ([http://chemdb2.niaid.nih.gov/struct\\_search/ivt/ivt\\_search.asp](http://chemdb2.niaid.nih.gov/struct_search/ivt/ivt_search.asp)). Since NAPETA represents a different type of inhibitor in comparison to the classic NNRTIs, it may be used as a lead to develop novel drugs against RT which could resist many of the mutations observed today when administering the classic NNRTIs. We plan to further investigate this inhibitor by testing its ability to protect human cells from HIV-1 infection.

## ACKNOWLEDGMENT

We deeply thank Prof. A. Nudelman for useful suggestions to the manuscript, Dr. S. H. Hughes from the National Cancer Institute for sending the plasmids that express the mutant HIV-1 RTs, studied here, Dr. A. N. Jain for kindly supplying Suflex, Open eye software for supplying Omega, and Dr. O. Mandelboim for the 721.221 cells. We also thank the following people from our laboratory: L. Guttmann for supplying the recombinant wild-type HIV-1 RT enzyme, O. Avidan for the recombinant PERV RT, and N. Kirshenboim for the recombinant TF1 RT. We are also grateful to the AIDS Research and Reference Reagent Program, Division of AIDS, National Institute of Allergy and Infectious Diseases, National Institutes of Health, for nevirapine and efavirenz.

## REFERENCES

- Coffin, J. M., Hughes, S. H., and Varmus, H. E. (1997) *Retroviruses*, Cold Spring Harbor Laboratory Press, Plainview, NY.
- De Clercq, E. (2004) Antiviral drugs in current clinical use, *J. Clin. Virol.* 30, 115–133.
- Das, K., Lewi, P. J., Hughes, S. H., and Arnold, E. (2005) Crystallography and the design of anti-AIDS drugs: Conformational flexibility and positional adaptability are important in the design of non-nucleoside HIV-1 reverse transcriptase inhibitors, *Prog. Biophys. Mol. Biol.* 88, 209–231.
- Ren, J., Diprose, J., Warren, J., Esnouf, R. M., Bird, L. E., Ikemizu, S., Slater, M., Milton, J., Balzarini, J., Stuart, D. I., and Stammers, D. K. (2000) Phenylethylthiazolylthiourea (PETT) non-nucleoside inhibitors of HIV-1 and HIV-2 reverse transcriptases. Structural and biochemical analyses, *J. Biol. Chem.* 275, 5633–5639.
- De Clercq, E. (2004) HIV-chemotherapy and -prophylaxis: New drugs, leads and approaches, *Int. J. Biochem. Cell Biol.* 36, 1800–1822.
- Sarafianos, S. G., Das, K., Hughes, S. H., and Arnold, E. (2004) Taking aim at a moving target: Designing drugs to inhibit drug-resistant HIV-1 reverse transcriptases, *Curr. Opin. Struct. Biol.* 14, 716–730.
- Das, K., Clark, A. D., Jr., Lewi, P. J., Heeres, J., De Jonge, M. R., Koymans, L. M., Vinkers, H. M., Daeyaert, F., Ludovici, D. W., Kukla, M. J., De Corte, B., Kavash, R. W., Ho, C. Y., Ye, H., Lichtenstein, M. A., Andries, K., Pauwels, R., De Bethune, M. P., Boyer, P. L., Clark, P., Hughes, S. H., Janssen, P. A., and Arnold, E. (2004) Roles of conformational and positional adaptability in structure-based design of TMC125-R165335 (etravirine) and related non-nucleoside reverse transcriptase inhibitors that are highly potent and effective against wild-type and drug-resistant HIV-1 variants, *J. Med. Chem.* 47, 2550–2560.
- Masuda, N., Yamamoto, O., Fujii, M., Ohgami, T., Fujiyasu, J., Kontani, T., Moritomo, A., Orita, M., Kurihara, H., Koga, H., Kageyama, S., Ohta, M., Inoue, H., Hatta, T., Shintani, M., Suzuki, H., Sudo, K., Shimizu, Y., Kodama, E., Matsuoka, M., Fujiwara, M., Yokota, T., Shigeta, S., and Baba, M. (2005) Studies of non-nucleoside HIV-1 reverse transcriptase inhibitors. Part 2: Synthesis and structure-activity relationships of 2-cyano and 2-hydroxy thiazolidenebenzenesulfonamide derivatives, *Bioorg. Med. Chem.* 13, 949–961.
- Romines, K. R., Freeman, G. A., Schaller, L. T., Cowan, J. R., Gonzales, S. S., Tidwell, J. H., Andrews, C. W., III, Stammers, D. K., Hazen, R. J., Ferris, R. G., Short, S. A., Chan, J. H., and Boone, L. R. (2006) Structure-activity relationship studies of novel benzophenones leading to the discovery of a potent, next generation HIV nonnucleoside reverse transcriptase inhibitor, *J. Med. Chem.* 49, 727–739.
- Janssen, P. A., Lewi, P. J., Arnold, E., Daeyaert, F., de Jonge, M., Heeres, J., Koymans, L., Vinkers, M., Guilleumont, J., Pasquier, E., Kukla, M., Ludovici, D., Andries, K., de Bethune, M. P., Pauwels, R., Das, K., Clark, A. D., Jr., Frenkel, Y. V., Hughes, S. H., Medaer, B., De Knaep, F., Bohets, H., De Clerck, F., Lampo, A., Williams, P., and Stoffels, P. (2005) In search of a novel anti-HIV drug: Multidisciplinary coordination in the discovery of 4-[[4-[[4-[(1E)-2-cyanoethenyl]-2,6-dimethylphenyl]-amino]-2-pyrimidinyl]amino]benzonitrile (R278474, rilpivirine), *J. Med. Chem.* 48, 1901–1909.
- Skillman, A. G., Maurer, K. W., Roe, D. C., Stauber, M. J., Eargle, D., Ewing, T. J., Muscate, A., Davioud-Charvet, E., Medaglia, M. V., Fisher, R. J., Arnold, E., Gao, H. Q., Buckheit, R., Boyer, P. L., Hughes, S. H., Kuntz, I. D., and Kenyon, G. L. (2002) A novel mechanism for inhibition of HIV-1 reverse transcriptase, *Bioorg. Chem.* 30, 443–458.
- Wang, L. Z., Kenyon, G. L., and Johnson, K. A. (2004) Novel mechanism of inhibition of HIV-1 reverse transcriptase by a new non-nucleoside analog, KM-1, *J. Biol. Chem.* 279, 38424–38432.
- Marchand, B., Tchesnokov, E. P., and Gotte, M. (2007) The pyrophosphate analogue foscarnet traps the pre-translocational state of HIV-1 reverse transcriptase in a Brownian ratchet model of polymerase translocation, *J. Biol. Chem.* 282, 3337–3346.
- Jochmans, D., Deval, J., Kesteleyn, B., Van Marck, H., Bettens, E., De Baere, I., Dehertogh, P., Ivens, T., Van Ginderen, M., Van Schoubroeck, B., Ehteshami, M., Wigerinck, P., Gotte, M., and Hertogs, K. (2006) Indolopyridones inhibit human immunodeficiency virus reverse transcriptase with a novel mechanism of action, *J. Virol.* 80, 12283–12292.
- Ren, J., Milton, J., Weaver, K. L., Short, S. A., Stuart, D. I., and Stammers, D. K. (2000) Structural basis for the resilience of efavirenz (DMP-266) to drug resistance mutations in HIV-1 reverse transcriptase, *Structure* 8, 1089–1094.
- Jain, A. N. (2003) Surflex: Fully automatic flexible molecular docking using a molecular similarity-based search engine, *J. Med. Chem.* 46, 499–511.
- Halgren, T. A. (1999) MMFF VII. Characterization of MMFF94, MMFF94s and other widely available force fields for conformational energies and for intermolecular interaction energies and geometries, *J. Comput. Chem.* 20, 730–748.
- Sevilya, Z., Loya, S., Adir, N., and Hizi, A. (2003) The ribonuclease H activity of the reverse transcriptases of human



- immunodeficiency viruses type 1 and type 2 is modulated by residue 294 of the small subunit, *Nucleic Acids Res.* **31**, 1481–1487.
19. Sevilya, Z., Loya, S., Hughes, S. H., and Hizi, A. (2001) The ribonuclease H activity of the reverse transcriptases of human immunodeficiency viruses type 1 and type 2 is affected by the thumb subdomain of the small protein subunits, *J. Mol. Biol.* **311**, 957–971.
  20. Kirshenboim, N., Hayouka, Z., Friedler, A., and Hizi, A. (2007) Expression and characterization of a novel reverse transcriptase of the LTR retrotransposon Tfl, *Virology* **366**, 263–276.
  21. Avidan, O., Loya, S., Tonjes, R. R., Sevilya, Z., and Hizi, A. (2003) Expression and characterization of a recombinant novel reverse transcriptase of a porcine endogenous retrovirus, *Virology* **307**, 341–357.
  22. Hizi, A., Tal, R., Shaharabany, M., Currens, M. J., Boyd, M. R., Hughes, S. H., and McMahon, J. B. (1993) Specific inhibition of the reverse transcriptase of human immunodeficiency virus type 1 and the chimeric enzymes of human immunodeficiency virus type 1 and type 2 by nonnucleoside inhibitors, *Antimicrob. Agents Chemother.* **37**, 1037–1042.
  23. Hizi, A., and Joklik, W. K. (1977) RNA-dependent DNA polymerase of avian sarcoma virus B77. I. Isolation and partial characterization of the  $\alpha$ ,  $\beta_2$ , and  $\alpha\beta$  forms of the enzyme, *J. Biol. Chem.* **252**, 2281–2289.
  24. DeLean, A., Munson, P. J., and Rodbard, D. (1978) Simultaneous analysis of families of sigmoidal curves: Application to bioassay, radioligand assay, and physiological dose-response curves, *Am. J. Physiol.* **235**, E97–E102.
  25. Roehm, N. W., Rodgers, G. H., Hatfield, S. M., and Glasebrook, A. L. (1991) An improved colorimetric assay for cell proliferation and viability utilizing the tetrazolium salt XTT, *J. Immunol. Methods* **142**, 257–265.
  26. Avidan, O., Meer, M. E., Oz, I., and Hizi, A. (2002) The processivity and fidelity of DNA synthesis exhibited by the reverse transcriptase of bovine leukemia virus, *Eur. J. Biochem.* **269**, 859–867.
  27. Bakhanashvili, M., and Hizi, A. (1994) Interaction of the reverse transcriptase of human immunodeficiency virus type 1 with DNA, *Biochemistry* **33**, 12222–12228.
  28. Nissley, D. V., Radzio, J., Ambrose, Z., Sheen, C. W., Hamamouch, N., Moore, K. L., Tachedjian, G., and Sluis-Cremer, N. (2007) Characterization of novel non-nucleoside reverse transcriptase (RT) inhibitor resistance mutations at residues 132 and 135 in the 51 kDa subunit of HIV-1 RT, *Biochem. J.* **404**, 151–157.
  29. Genin, M. J., Biles, C., Keiser, B. J., Poppe, S. M., Swaney, S. M., Tarpley, W. G., Yagi, Y., and Romero, D. L. (2000) Novel 1,5-diphenylpyrazole nonnucleoside HIV-1 reverse transcriptase inhibitors with enhanced activity versus the delavirdine-resistant P236L mutant: Lead identification and SAR of 3- and 4-substituted derivatives, *J. Med. Chem.* **43**, 1034–1040.
  30. Pelemans, H., Esnouf, R. M., Parniak, M. A., Vandamme, A. M., De Clercq, E., and Balzarini, J. (1998) A proline-to-histidine substitution at position 225 of human immunodeficiency virus type 1 (HIV-1) reverse transcriptase (RT) sensitizes HIV-1 RT to BHAP U-90152, *J. Gen. Virol.* **79**, 1347–1352.
  31. Brandt, R. B., Laux, J. E., and Yates, S. W. (1987) Calculation of inhibitor  $K_i$  and inhibitor type from the concentration of inhibitor for 50% inhibition for Michaelis-Menten enzymes, *Biochem. Med. Metab. Biol.* **37**, 344–349.
  32. Lipinski, C. A., Lombardo, F., Dominy, B. W., and Feeney, P. J. (2001) Experimental and computational approaches to estimate solubility and permeability in drug discovery and development settings, *Adv. Drug Delivery Rev.* **46**, 3–26.
  33. Oz Gleenberg, I., Herschhorn, A., Goldgur, Y., and Hizi, A. (2007) Inhibition of human immunodeficiency virus type-1 reverse transcriptase by a novel peptide derived from the viral integrase, *Arch. Biochem. Biophys.* **458**, 202–212.
  34. Herschhorn, A., Lerman, L., Weitman, M., Gleenberg, I. O., Nudelman, A., and Hizi, A. (2007) De novo parallel design, synthesis and evaluation of inhibitors against the reverse transcriptase of human immunodeficiency virus type-1 and drug-resistant variants, *J. Med. Chem.* **50**, 2370–2384.
  35. Doman, T. N., McGovern, S. L., Witherbee, B. J., Kasten, T. P., Kurumbail, R., Stallings, W. C., Connolly, D. T., and Shoichet, B. K. (2002) Molecular docking and high-throughput screening for novel inhibitors of protein tyrosine phosphatase-1B, *J. Med. Chem.* **45**, 2213–2221.
  36. Cruchaga, C., Anso, E., Font, M., Martino, V. S., Rouzaut, A., and Martinez-Irujo, J. J. (2007) A new strategy to inhibit the excision reaction catalysed by HIV-1 reverse transcriptase: compounds that compete with the template-primer, *Biochem. J.* **405**, 165–171.

BI7018139